DEUTSCHES ELEKTRONEN-SYNCHROTRON DESY

DESY SR-77/03
January 1977

Calibration of Radiometric Transfer Standards in the UV and VUV by Electron Synchrotron Radiation Using a Normal Incidence Radiometer

by

D. Einfeld, D. Stuck and B. Wende
Physikalisch-Technische Bundesanstalt
Institut Berlin
Abbestraße 2-12
1000 Berlin

NOTKESTRASSE 85 · 2 HAMBURG 52

CALIBRATION OF RADIOMETRIC TRANSFER STANDARDS IN THE UV AND VUV BY ELECTRON SYNCHROTRON RADIATION USING A NORMAL INCIDENCE RADIOMETER

D. Einfeld, D. Stuck and B. Wende
Physikalisch-Technische Bundesanstalt, Institut Berlin
Abbestraße 2 - 12, 1000 Berlin

Submitted to Int. J. Scient. Metrology

Abstract

In order to utilize the electron synchrotron radiation for the calibration of radiometric transfer standards a radiometer has been developed which is in use at the Deutsches Elektronen-Synchrotron (DESY, Hamburg). The radiometer is designed for calibrating transfer standards of the spectral radiance and irradiance for wavelengths between 80 nm and 350 nm. By the used method it is avoided that after calibration with synchrotron radiation the transfer standards have to be converted to an absolute scale by comparing them with a conventional standard in the uv. This is especially vital for those vuv standards which do not emit any measurable radiation in the uv. In this paper the quality of the underlying principle of measurement is stressed by determining the spectral radiance of commercial deuterium lamps (165 nm to 340 nm). The uncertainty of the measured spectral radiance is ± 2 %. This uncertainty is confirmed by comparative measurements (290 nm to 340 nm) based on the radiation of tungsten tube blackbody at the temperature of about 2500 K.

Contents:

1. Introduction

1.1 Radiometric Techniques in the UV and VUV and Their Fields of Application

To determine spectral radiant quantities (radiance, irradiance or radiant flux) the respective source is usually compared with a radiometric standard. In the wavelength region between 300 nm and 2500 nm blackbody radiators are known to be well established radiometric standards. The relative uncertainties of transfer standards e. g. for the spectral radiance (tungsten strip lamps) is 10^{-2} at 300 nm, $0.6\cdot10^{-2}$ between 400 nm and 1000 nm, and $2.5\cdot10^{-2}$ at 2500 nm (see section 5.5). For wavelengths of about 250 nm and below, however, well checked radiometric standards with uncertainties (in spectral radiance) of the order of ± 1 % to ± 5 % are missing up to now. Particularly in plasmaphysics transfer standards of the spectral radiance are required, such as for thermonuclear fusion research [1], for the measurement of plasma spectroscopic parameters [2], and for establishing a temperature scale [3-5], while in other fields of research transfer standards of the spectral irradiance are more important (e. g. in solid state physics, photochemistry, biology, medicine).

Detectors calibrated below 250 nm are well studied [6]. The use of detectors with known spectral response for the calibration of radiation standards, however, has the significant disadvantage that the transmission factor of the radiometric apparatus has to be measured accurately. Such measurements with small uncertainties have not been achieved so far. They are made particularly difficult in the vuv region because the transmission factor is often subject to fast alterations. At present, it is thus more advisable to calibrate radiation standards by a radiometric comparison with a source of known (that means precisely calculable) spectral radiant power.

To this purpose different kinds of radiation sources in the vuv have been used so far: the electron synchrotron radiation [7], the plasma blackbody radiation of known temperature [8, 9], the radiation of a wall stabilized steady state hydrogen plasma [10], and gas discharges in connection with the branching ratio technique [11]. In comparison with a synchrotron the aforementioned sources have certain disadvantages, for they are restricted to a limited spectral region, and because it is necessary to use assumptions on the properties of the sources which are not yet completely checked out.

1.2 Motivation of This Work

Synchrotron radiation has been studied in [7, 9, 12, 13, 14] with respect to the development of calibration procedures. But only in [7, 9] the more difficult vuv region has been treated.

PITZ [7] measured the spectral radiance of deuterium lamps between 165 nm and 270 nm, while STUCK and WENDE [9] calibrated microwave powered xenon discharges between 165 nm and 185 nm using PITZ' equipment. With the transfer standards it had been demonstrated that at $\lambda = 165$ nm calibrations with the synchrotron radiation on the one hand and plasma blackbody radiation on the other agree upon each other within 8 % [9]. For the region between 165 nm and 255 nm deuterium lamps calibrated with respect to the hydrogen continuum of an arc plasma agreed within 10 % with those calibrated by PITZ at the synchrotron, while between 255 nm and 270 nm a systematic error of about 25 % may have affected the PITZ calibration [15].

In order to decide whether the found discrepancy is of any significance or just due to the used arrangements it appeared to be necessary therefore, to develop an improved technique for the radiometric utilization of electron synchrotron radiation. A possible disadvantage of the early measurements may be the fact that an additional mirror is used when the synchrotron radiation is compared to that of the transfer standards. In order to evaluate the final calibration results the reflection factor of the mirror has to be measured. This might cause errors, for specifically in the vuv an accurate determination of the

reflection factor requires great effort. In particular it is also subject to fast alterations.
With the radiometer developed for this work and being presently in use at the Deutsches Elektronen-Synchrotron (DESY, Hamburg) this disadvantage has been avoided. The radiometer was designed for calibrating transfer standards (spectral radiance and irradiance) for wavelengths between 80 nm and 350 nm. In this paper the quality of the underlying principle of measurement is stressed by determining the spectral radiance of commercial deuterium lamps, and the estimated systematic uncertainties are confirmed by comparative measurements.
Deuterium lamps are useful as transfer standards, because they emit for $\lambda > 165$ nm a line-free continuum, are cheaply procurable, and convenient to operate. A disadvantage is that their spectral radiance decreases with increasing time of operation, so that further work will be necessary in order to introduce them as very reliable transfer standards. But these topics are not subject of the present work.

2. Properties of the Electron Synchrotron Radiation at DESY Relevant for the Calibration Procedure

It shall be avoided here to present the underlying theory of electron synchrotron radiation due to Schwinger [16] which can be found in several review papers (e. g.: [17, 18]. The main properties of the radiation of an electron synchrotron can be summarized as follows:

1. The emitted spectral radiant power is calculable and depends on known machine parameters such as the orbital radius, the mode of acceleration of the electrons and their final energy.
2. The radiated power is proportional to the number of accelerated electrons.
3. The spectral distribution of the radiation is continuous and covers a wide spectral range from the IR- to the X-ray wavelength region depending on the electron energy.
4. The radiation is confined to a narrow band near the synchrotron orbital plane.
5. The synchrotron radiation is eliptically polarized.

In order to utilize synchrotron radiation for a radiometric calibration procedure the Schwinger theory is applied with respect to the machine parameters of DESY. In the experimental arrangement to be described later an aperture stop is posed in a distance $D = 40.08$ m from the tangent point on the electron orbit as shown in Fig. 1. With two rectangularlike apertures 1 and 2 (height $a = 4$ mm, width $b = 10$ mm) two beams are isolated (beam 1 above and beam 2 below the synchrotron orbital plane). The direction of the beams is characterized by the azimuthal angles Ψ or by the positions z in the plane of the aperture stop. It is Ψ the angle between the beam's direction and its projection onto the synchrotron orbital plane, z being defined by $z = D \cdot \Psi$. In Fig. 2 the spectral radiant power Φ_λ^{Sy} calculated for conditions as used at DESY is plotted over Ψ or z respectively. Φ_λ^{Sy} is the mean value taken over $t_2 - t_1 = 2$ ms of that part of the synchrotron radiation passing through aperture 1. The integration starts at $t_1 = 4$ ms after injection of the electrons to be accelerated. The total acceleration time of the electrons is 10 ms and the final energy amounts to 6 GeV. For the wavelengths between 100 nm and 550 nm the function Φ_λ^{Sy} increases slightly with increasing Ψ. After reaching the maximum values at angles between $\Psi \approx 0.5$ and 1.5 mrad Φ_λ^{Sy} decreases strongly with further increase of Ψ. From the angular distribution of Fig. 2 one can conclude that especially that part of the synchrotron radiation is appropriate for the calibration procedure which is in the vicinity of the synchrotron orbital plane ($\Psi = 0$). In this case uncertainties of Φ_λ^{Sy} produced by not exactly adjusted apertures 1 and 2 are minimized.

The degree of polarization of the synchrotron radiation demands a careful attention. Carrying out a radiometric comparison between sources of different degree of polarization $p(\lambda)$ (e. g. between a synchrotron ($p(\lambda) \neq 0$) and a gas discharge ($p(\lambda) \cong 0$)) a wavelength dependent transmission factor of the used radiometer has to be considered caused by the different reflection factors of the optical elements in the two perpendicular directions of the electrical vector. Angular distributions of the degrees of polarization of the synchrotron radiation are shown in Fig. 3 having been computed under the same conditions as mentioned above for Φ_λ^{Sy}. $p(\lambda)$ represents mean values with respect to the spatial integration (height of aperture 1; 4 mm) and the temporal one (integration time: 2 ms). The radiation is completely plane polarized in the synchrotron orbital plane $\Psi = 0$ with the electrical vector parallel to the synchrotron orbital plane.

3. Principle of Measurement

The spectral radiant power Φ^{Sy}_{λ} displayed in Fig. 2 is proportional to the number of electrons in orbit. This electron number varies during the acceleration time and differs considerably from acceleration cycle to acceleration cycle. For the vuv calibration procedure a method has been used therefore which is independent of the number of electrons in orbit. According to a proposal of LEMKE and LABS [12] this method requires simultaneous measurements of the synchrotron radiation in both the visible and vuv spectral regions. We assume that beam 1 shown in Fig. 1 passes through a radiometric device which is adjusted at a fixed wavelength λ_o in the visible spectral region, while beam 2 is passing through a similar device, which can be adjusted at an arbitrary wavelength λ in the vuv spectral region. The spectrally decomposed radiation is measured with photomultipliers, one each for the visible and vuv respectively. The mean values of the corresponding photomultiplier current taken over the time $t_2 - t_1$ are $i^{Sy}(\lambda)$ and $i^{Sy}(\lambda_o)$. Their ratio is

$$\frac{i^{Sy}(\lambda)}{i^{Sy}(\lambda_o)} = \frac{s^{vuv}(\lambda)}{s^{vis}(\lambda_o)} \cdot \frac{1+p^{Sy}(\lambda)\cdot p^{vuv}(\lambda)}{1+p^{Sy}(\lambda_o)\cdot p^{vis}(\lambda_o)} \cdot \frac{\tilde{\Phi}^{Sy}_{\lambda}(\lambda)}{\tilde{\Phi}^{Sy}_{\lambda}(\lambda_o)} \qquad (1)$$

In Eq. 1 s means the sensitivity of the radiometric device with respect to unpolarized radiation, which is given by its transmission factor, its spectral bandwidth and by the photomultiplier response, p the degree of polarization produced by the device, p^{Sy} the degree of polarization of the synchrotron radiation, $\tilde{\Phi}^{Sy}_{\lambda}(\lambda)$ the radiant power per electron in orbit. In Eq. 1 a suffix vuv and/or a λ in brackets denote quantities in the vuv spectral region, while vis and/or λ_o respectively denote those in the visible. The measurements of $i^{Sy}(\lambda)/i^{Sy}(\lambda_o)$ determine $s^{vuv}(\lambda)/s^{vis}(\lambda_o)$ according to Eq. 1.

After having determined the left hand side of Eq. 1 in a subsequent measurement, the unpolarized radiation of a calibrated tungsten strip lamp passes through aperture 1 while that of a vuv transfer standard to be calibrated passes through aperture 2. The ratio of the corresponding photomultiplier currents is of the form

$$\frac{i^{vuv}(\lambda)}{i^{TSL}(\lambda_o)} = \frac{s^{vuv}(\lambda)}{s^{vis}(\lambda_o)} \cdot \frac{\Phi^{vuv}_{\lambda}}{\Phi^{TSL}_{\lambda}} , \qquad (2)$$

where Φ^{TSL}_{λ} means the spectral radiant power of the tungsten strip lamp radiation passing through aperture 1. Φ^{vuv}_{λ} means the power with respect to vuv transfer standard; $i^{vuv}(\lambda)$ and $i^{TSL}(\lambda_o)$ are the corresponding photomultiplier currents which need not necessarily to be measured simultaneously. In the case that during the measurements of the tungsten strip lamp and the vuv transfer standard the solid angle and the emitting area are of equal size we have

$$\frac{\Phi_\lambda^{vuv}}{\Phi_\lambda^{TSL}} = \frac{L_\lambda^{vuv}}{L_\lambda^{TSL}} \quad , \tag{3}$$

where L_λ^{vuv} is the unknown spectral radiance of the vuv transfer standard and L_λ^{TSL} the known one of the tungsten strip lamp. With Eqs. 1 to 3 follows

$$L_\lambda^{vuv} = \frac{i^{Sy}(\lambda_o)}{i^{Sy}(\lambda)} \cdot \frac{i^{vuv}(\lambda)}{i^{TSL}(\lambda_o)} \, L_\lambda^{TSL}(\lambda_o) \cdot F(\lambda) \tag{4}$$

$$F(\lambda) = \frac{1 + p^{Sy}(\lambda)\, p^{vuv}(\lambda)}{1 + p^{Sy}(\lambda_o)\, p^{vis}(\lambda_o)} \cdot \frac{\tilde{\Phi}_\lambda^{Sy}(\lambda)}{\tilde{\Phi}_\lambda^{Sy}(\lambda_o)}$$

on which the measurement of L_λ^{vuv} is based. The photomultiplier currents $i^{Sy}(\lambda_o)$ and $i^{Sy}(\lambda)$ corresponding to synchrotron radiation in Eq. 4 have to be measured simultaneously. $i^{vuv}(\lambda)$ and $i^{TSL}(\lambda_o)$ can be determined short before or after the synchrotron radiation measurements. Between the measurements, however, it has to be avoided severely to change the transmission factor and the bandwidths of the radiometric devices as well as the response of the photomultipliers.

The expression $F(\lambda)$ is determined by the properties of the used synchrotron radiation source and by the degree of polarization $p^{vuv}(\lambda)$ and $p^{vis}(\lambda_o)$ produced by the radiometric devices. Measurements of the latter quantities are described in section 5.2. In Fig. 4 the function $F(\lambda)$ is plotted over the wavelength for final energies between 1.7 GeV and 7.2 GeV of the electrons accelerated at DESY. $F(\lambda)$ has been calculated for conditions of the final measurements. Aperture 1 as shown in Figs. 1 and 7 (vis-channel) is located with its center at a position $z = 6$ mm above the synchrotron orbital plane and aperture 2 (vuv-channel) at $z = -18$ mm below the synchrotron orbital plane. The wavelength λ_o is chosen to be 458 nm. In Fig. 4 one recognizes that $F(\lambda)$ increases strongly with decreasing wavelength. For final energies larger than 3.5 GeV the function $F(\lambda)$ varies only slightly. Above 3.5 GeV the calibration procedure according to Eq. 4 is therefore nearly independent upon the final energy of the electrons.

4. Apparatus

4.1 Optical Arrangement of the Radiometer

To perform calibrations according to Eq. 4 a special radiometric device has been set up (Fig. 5). The main optical components of this radiometer are a concave mirror (focal length: f = 400 mm) and two 0.5 m-Seya-Namioka monochromators having a pinhole of 0.45 mm in diameter acting as common entrance slit, but having separate exit slits and photoelectric detectors. The plate factor of both monochromators is 1.7 nm/mm (gratings: 1200 lines per mm). The optical axes of the monochromators are running nearly inside the orbital plane of the synchrotron. The concave mirror can be placed in position A as well as in B. When the concave mirror is in A, the synchrotron radiation is focussed onto the entrance pinhole. In this case the distance between the concave mirror and the observed part of the electron beam of the synchrotron is 40.08 m (due to reasons of safety and construction). In order to measure the radiation of the vuv-transfer standards and the tungsten strip lamp the concave mirror is moved from A to B. Then, the emitting areas of the standards are imaged onto the common entrance pinhole of the monochromators (being reduced by one half). In this case the distance between the concave mirror and the transfer standards is 1.2 m.

The synchrotron radiation impinging onto the concave mirror is

splitted by the aperture stop into two beams running spatially above each other. The radiation coming from the lower aperture (aperture 2) enters the vuv-monochromator unaffected by the entrance pinhole and is measured photoelectrically (multiplier: EMI 9558 QB, S-20 cathode) after its spectral decomposition by the vuv-grating (blaze wavelength $\lambda = 150$ nm). Concave mirror and grating are evaporated with aluminium and overcoated with MgF_2. X-ray radiation propagating in the vicinity of the synchrotron plane is blocked out by a shutter in front of the radiometer (not shown in Fig. 5, compare Fig. 7). The influence of stray-light and radiation of higher orders overlapping the first order spectrum has been studied by using interference filters placed behind the exit slit and by using the photomultiplier EMR 541F-05M-14, which is sensitive in the limited spectral range between 145 nm and 345 nm. Between 160 nm and 345 nm the portion of that radiation falsifies the photomultiplier currents by 0.1 %.

The synchrotron radiation originating at the upper aperture (aperture 1) of the concave mirror enters the vis-monochromator, is separated spatially from the beam in the vuv-monochromator behind the entrance pinhole by two plane mirrors, and is measured photoelectrically (multiplier: EMI 9558 QB, S-20 cathode) after its spectral decomposition by the vis-grating (blaze wavelength: $\lambda = 560$ nm). An interference filter with the peak wavelength λ_o = 458 nm is used to suppress stray-light and radiation of higher orders overlapping the first order spectrum. In order to measure the ratio $i^{Sy}(\lambda_o)/i^{Sy}(\lambda)$ of Eq. 4 the vis-monochromator is adjusted at the fixed wavelength λ_o = 458 nm, while the vuv-monochromator is scanned through the wavelength range in which the vuv-transfer standards shall be calibrated.

In order to measure the photomultiplier current $i^{vis}(\lambda_o)$ of Eq. 4 the aperture 1 of the concave mirror is irradiated by a calibrated tungsten strip lamp. This measurement is performed after the concave mirror has been moved by 200 mm from the initial position A to position B and has been turned around the z-axis by 3.6° and shifted by 6 mm in the z-direction (the latter being perpendicular to the plane defined by the entrance pinhole and the centers of the concave mirror, gratings, and exit slits).

Subsequently, the aperture 2 of the concave mirror is irradiated by the vuv-transfer standards for the measurement of the photomultiplier current $i^{vuv}(\lambda)$ of Eq. 4. In this case the concave mirror itself is shifted by 12 mm in the (-z)-direction with respect to the above mentioned position B. By this shifting in the ($\pm$ z)-directions it is achieved that only such surfaces of the gratings and plane mirrors are used for the measurement of the tungsten strip lamp and the vuv-transfer standards which are

also used for measurement of the synchrotron radiation. This condition is of vital nature, for the efficiency of the gratings decreases more rapidly by irradiation due to synchrotron radiation than by radiation due to the tungsten strip lamp and the vuv-transfer standards. By the chosen principle of measurement it cannot be completely avoided that the irradiated surfaces of the gratings used with the synchrotron radiation are larger than those used with the radiation of the tungsten strip lamp and the vuv-transfer standards respectively (see analysis of uncertainties, section 5.4).

The above mentioned adjustments of the concave mirror have been carried out frequently under vacuum conditions and remote control. Reproducibility of this was so well achieved that realignment of the optical arrangement was not necessary even during long-term experimental periods of several months. It has been of advantage, that the vis-monochromator could be scanned in the same way as the vuv-monochromator in order to check the whole arrangement. It could be shown that by adjusting both monochromators at the same wavelengths in the near uv the radiometer and the synchrotron behaved in agreement with Eq. 4 (using for measuring $i^{vuv}(\lambda)$ and $i^{TSL}(\lambda_o)$ the radiation of a tungsten strip lamp).

To determine the degree of polarization produced by the radiometer polarizers have been attached in front of the exit slits of the vuv-monochromator and of the vis-monochromator.

4.2 Vacuum Equipment

The optical elements of the radiometer are mounted on a cast iron base inserted in a stainless steel vacuum tank (volume $\approx$700 l). Two turbomolecular pumping units having a pumping speed of 270 l/s each evacuate the tank. Despite the 6 small electric motors and corresponding current-carrying wires inside the tank which are used for adjustments and movements of the optical elements, the working pressure of 10^{-3} Pa ($\approx 10^{-5}$ torr) is already reached at about 6 hours. The final pressure of 10^{-5} Pa is reached after several weeks pumping time. The vuv-transfer standard and the tungsten strip lamp are mounted outside the vacuum tank, and it is possible to exchange them without venting the tank.

4.3 Device for measuring photomultiplier currents

The photomultiplier currents of the vis- and vuv-photomultiplier are measured by two identical electronic devices both being synchronized by a trigger pulse which is started at the time of injection of the electrons to be accelerated. These devices permit measurements of the radiant power of the relevant parts

of the synchrotron radiation pulses by using for the determination of the photomultiplier currents a preselected time interval (according to the trigger pulse) with both variable delay and variable gate time (delay $\Delta t'$ = 0, 1, 2, ..., 9 ms; gate time Δt = 1, 2, 5, and 10 ms). The latter time interval of 10 ms is the total acceleration time of the synchrotron electrons. Delay and gate time are set in such a manner that only those parts of the synchrotron radiation pulses are used for which approximately no variation in time of the radiant power exists (Fig. 6a). Usually the delay time was $\Delta t' = 4$ ms and the gate time $\Delta t = 2$ ms.

Some details of the electronic device are shown in Fig. 6b. The photomultiplier current is processed in the usual way with a current-voltage converter (time constant $\approx 1\,\mu s$), then scanned during the gate time with a sample-and-hold amplifier in a 20 kHz mode and fed into an analog-digital converter. For a preselected number of synchrotron pulses (10^m, m = 1, 2, 3, 4) the mean values of the photomultiplier currents of the single pulses are summed, then displayed and fed into a small computer. The photomultiplier currents corresponding to synchrotron radiation and to the radiation of the transfer standards have been measured using identical gate time and duty cycle. For almost all measurements the photomultiplier currents have been smaller than $5\cdot10^{-8}$ A, only in some cases they increased to $5\cdot10^{-7}$ A. Typical ratios of the photomultiplier currents varied between 1:2 and 1:5. The relative uncertainty of these ratios produced by the electronic device described above is $< 10^{-3}$.

5. Results

5.1 Adjustment of the Radiometer with Respect to the Synchrotron Radiation Field

The radiometer is connected with the vacuum chamber of the synchrotron by a vacuum tube of about 40 m length and of 50 mm inner diameter containing beam stops for the suppression of wall reflections. Before running the calibration experiments the concave mirror with the aperture stop (working position A in Fig. 5) is placed symmetrically into the available synchrotron radiation field by shifting the whole arrangement. The correct irradiation of apertures 1 and 2 of the aperture stop in front of the concave mirror is checked by photographing the synchrotron radiation field. To this purpose the concave mirror is substituted by a camera. Apertures 1 and 2, the axis of symmetry of the synchrotron radiation field and the position of the synchrotron plane which is located 6 mm above the axis of symmetry, are all drawn into the photograph of the synchrotron radiation field (Fig. 7a). In Fig. 7b the available synchrotron radiation field is presented if using the shutter to block out the x-ray radiation propagating in the vicinity of the synchrotron plane.

The position of the synchrotron plane is measured by taking a plastic foil adjusted in front of the concave mirror. The part of the foil exposed to x-ray radiation in the vicinity of the synchrotron plane is browned after an exposure time of a few seconds. This allows to determine the position of the synchrotron plane with an uncertainty of $\Delta z = \pm 0.5$ mm and the values of azimuthal angles Ψ_i ($\Psi_1 = 0.100$ mrad, $\Psi_2 = 0.200$ mrad, $\Psi_3 = 0.350$ mrad, $\Psi_4 = 0.450$ mrad) with an uncertainty of $\Psi_i = \pm 0.013$ mrad. Knowing the angles Ψ_i the synchrotron radiation energy impinging onto apertures 1 and 2 can be obtained from Fig. 1, its uncertainty being caused by the uncertainty of the angles Ψ_i (see also analysis of the uncertainties, section 5.4).

5.2 Polarization Behavior of the Radiometer

The evaluation of Eq. 4 requires measurements of the degree of polarization produced by the optical elements of the vis-channel and of the vuv-channel of the radiometer. For these measurements three types of polarizers are used

i two different types of film polarizers mounted between quartz plates, one manufactured by Käsemann, Germany, the other by Oriel, USA,

ii a LiF pile-of-plates polarizer with eight plates.

The polarization behavior of the used polarizers has to be determined (Tab. 1). The degree of polarization produced by the film polarizers has been measured in the usual way by using two identical polarizers. The degree of polarization produced by the LiF pile-of-plates polarizer has been computed within the spectral range between 105 nm and 350 nm using the optical constants n and k of LiF according to [19] and the equations given in [20] for single reflections. Additionally the degree of polarization produced by the LiF-polarizer has been measured between 260 nm and 350 nm using the film polarizers. The relative spectral dependence of the degree of polarization has been found to agree very well upon its measured and calculated values. The measured "absolute" values however, deviate by 13 % from the calculated ones. In the following therefore the computations serve exclusively the purpose of determining the relative spectral dependence of the degree of polarization of the LiF pile-of-plates polarizer. The "absolute" values of the spectral dependence have been determined by adapting them to the values measured between 260 nm and 350 nm.

The measured degree of polarization produced by the optical elements of the vis-channel and of the vuv-channel of the radiometer is presented in Fig. 8.

5.3 The Spectral Radiance of Deuterium Lamps

For the calibration procedure deuterium lamps manufactured by Quarzlampengesellschaft mbH, Hanau, Germany (type: D-60 F) have been chosen. The operating conditions laid down for the utilization of this lamps as radiometric transfer standards are completely given in [21], (compare also Fig. 9). According to Eq. 4 the spectral radiance of the deuterium lamps has been measured.

Because the spectral radiance of the deuterium lamps alters strongly with operating time (compare Tab. 2), it is useful to give the relative spectral radiance instead of the measured "absolute" one. Short before application by other users however, the lamps have to be converted to an absolute scale by a radiometric comparison with a calibrated tungsten strip lamp or low current carbon arc [22] at about 300 nm. The relative spectral radiances of lamps which had been purchased at the same time and had the same number of operating hours differed from each other by less than ± 5 %. As an example Fig. 9 shows the relative spectral radiance of three lamps after 50 operating hours. It is thus not always necessary for application purposes with a low demand of accuracy to measure the relative spectral radiance individually for each specimen.

Also the relative spectral radiance has not been constant during the lifetime of the lamps. The amount of alteration can be obtained from Fig. 10. Relative spectral radiances are displayed there for four groups of lamps with different numbers of operating hours. With increasing number of operating hours the maximum

of the spectral radiance is subject to a shift towards longer wavelength. As a guiding value it has been found by examination of 9 lamps that between 165 nm and 350 nm the relative spectral radiance alters by 5 % after 20 operating hours each time. For the four groups of lamps whose relative spectral radiances are presented in Fig. 10 the spectral radiances at $\lambda = 200$ nm are listed in Tab. 2. One can recognize the differences of the spectral radiance inside the groups and the decreasing of the spectral radiance with the number of operating hours. The observed alterations of the chosen deuterium lamps given in Fig. 10 and Tab. 2 demonstrate the fact that further work will be necessary in order to introduce them as very reliable transfer standards such that no repeated calibration is needed for long periods. Improved conditions of production and selection of the lamps, smaller heating and discharge currents could eventually establish further progress. But these investigations and developments were not subject of the present work.

Finally it may be mentioned that the given relative spectral radiances of the measured deuterium lamps must not be used for different types of lamps (Fig. 11).

5.4 Analysis of Uncertainties

The relative uncertainty of the measured spectral radiance L_λ^{vuv}

of the vuv transfer standards can be motivated according to Eq. 4 to be of the form

$$\left(\frac{\Delta L_\lambda^{vuv}}{L_\lambda^{vuv}}\right)^2 = \sum_{i=1}^{5}\left(\frac{\Delta y_i}{y_i}\right)^2 = \left\{\frac{\Delta\left(\frac{i^{Sy}(\lambda_0)}{i^{Sy}(\lambda)}\right)}{\frac{i^{Sy}(\lambda_0)}{i^{Sy}(\lambda)}}\right\}^2 + \left\{\frac{\Delta i^{vuv}}{i^{vuv}}\right\}^2 + \left\{\frac{\Delta i^{TSL}}{i^{TSL}}\right\}^2 + \left\{\frac{\Delta F(\lambda)}{F(\lambda)}\right\}^2 + \left\{\frac{\Delta L_\lambda^{TSL}}{L_\lambda^{TSL}}\right\}^2 \qquad (5)$$

The individual contributions $\Delta x_k^{(1)}/x_k^{(1)}$ to the five terms $\Delta y_i/y_i$ of this equation are separately displayed in Tab. 3 a to d. Some of them need further discussion.

The measured ratio of the photomultiplier currents $i^{Sy}(\lambda_0)/i^{Sy}(\lambda)$ is uncertain because of stray-light and higher orders overlapping the first order spectrum which results to $\Delta y_1/y_1 = 10^{-3}$. It may be of particular interest to mention that for final energies of the synchrotron electrons less than 6 GeV this contribution includes the amount of x-ray stray-light. Concerning the random uncertainty of the ratio $i^{Sy}(\lambda_0)/i^{Sy}(\lambda)$ the relative standard error of the mean is satisfactorily small (typically $5\cdot10^{-4}$ for five measurements). Further uncertainties influencing the ratio of the photomultiplier currents are covered by uncertainties of $i^{vuv}(\lambda)$ and $i^{TSL}(\lambda_0)$ (Tab. 3b).

The contribution to the uncertainty by non-linearity and drift of the photomultipliers is estimated to be about $1.5\cdot10^{-3}$. For the

photomultiplier EMI 9558 QB this has been determined using measurements according to [23]. For almost all measurements the photomultiplier currents have been smaller than $5\cdot10^{-8}$ A, in some cases they increased to $5\cdot10^{-7}$ A. Typical ratios of the photomultiplier currents varied between 1:2 and 1:5. A possible contribution to the uncertainty may be produced by the bunch structure of the synchrotron current. The bunch structure leads to synchrotron radiation pulses having a halfwidth of 0.3 ns and a duty cycle of 2 ns. The time spread of the used photomultiplier is of the order of 50 ns, so that in the neighbourhood of the anode averaged electron currents can be assumed in good approximation. We have taken into account therefore no additional non-linearity behavior caused by photocurrent pulses at the cathode due to the bunch structure. By the chosen principle of measurement it cannot be completely avoided that the irradiated areas of the gratings used with synchrotron radiation are larger than those used with the radiation of the tungsten strip lamp and the vuv transfer standards respectively. The uncertainty caused by that fact is described by "different size of the irradiated grating surface" (Tab. 3b), which takes into account spatial variations of the gratings' efficiencies. The term "diffraction" means that an uncertainty has to be considered which is caused by diffraction losses [24] having different amounts for the synchrotron radiation and for that of the transfer standards. A rough estimate of this contribution to the uncertainty is $\Delta x_k^{(2,3)}/x_k^{(2,3)} = \pm 5\cdot 10^{-3}$. During measurement of the synchrotron radiation the transmission factor of the radiometer alters slightly. This alteration however, does not contribute to the uncertainties, because the influence has been avoided by using a special sequence for measuring the photomultiplier currents $i^{Sy}(\lambda_o)$; $i^{Sy}(\lambda)$; $i^{vuv}(\lambda)$ and $i^{TSL}(\lambda_o)$.

In Tab. 3c the uncertainty contributions $\Delta x_k^{(4)}/x_k^{(4)}$ to $F(\lambda)$ are given, where $F(\lambda)$ is calculated according to the Schwinger theory assuming the synchrotron electrons to be on an ideally circular orbit. At DESY the electrons have a spatial distribution with a measured halfwidth perpendicular to the synchrotron orbital plane of 0.7 mm. The uncertainty contribution to $F(\lambda)$ by this perturbing influence has been estimated to be $\Delta x_k^{(4)}/x_k^{(4)} = \pm 2\cdot 10^{-3}$, assuming that the spatial distribution of the electrons is caused by betatron oscillations. The uncertainty $\Delta z = \pm 0.5$ mm of the positions of apertures 1 and 2 gives rise to an uncertainty contribution to $F(\lambda)$ of $\Delta x_k^{(4)}/x_k^{(4)} = \pm 6\cdot 10^{-3}$. The radius R of the electron orbit is uncertain by $\Delta R/R = \pm 1.5\cdot 10^{-3}$, the energy E by $\Delta E/E = \pm 10^{-2}$ which causes uncertainty contributions to $F(\lambda)$ of $\Delta x_k^{(4)}/x_k^{(4)} = 4\cdot 10^{-4}$ and $\Delta x_k^{(4)}/x_k^{(4)} = \pm 7\cdot 10^{-4}$ respectively. Finally the uncertainties $\Delta p^{vis} = \pm 0.8\cdot 10^{-2}$ and $\Delta p^{vuv} = \pm 1.5\cdot 10^{-2}$ of the degree of polarization produced by the radiometer in the visible and vuv contribute to the uncertainty of $F(\lambda)$ by $\Delta x_k^{(4)}/x_k^{(4)} = \pm 6\cdot 10^{-3}$ and $\Delta x_k^{(4)}/x_k^{(4)} = \pm 10^{-2}$ respectively.

The spectral radiance L_λ^{TSL} of the tungsten strip lamp measured by a radiometric comparison with a blackbody radiator is uncertain by $\Delta L_\lambda/L_\lambda = \pm 6\cdot 10^{-3}$ at $\lambda_c = 458$ nm (see section 5.5). Because of some unfavourable operating conditions during the comparisons with the synchrotron radiation this uncertainty had to be enlarged to $\pm 8\cdot 10^{-3}$.

If the mentioned five uncertainty terms $\Delta y_i/y_i$ are combined according to Eq. 5 the total uncertainty of the spectral radiance L_λ^{vuv} of the vuv transfer standards amounts to $\Delta L_\lambda^{vuv}/L_\lambda^{vuv} = \pm 1.8\cdot 10^{-2}$. It can be accepted therefore that transfer standards can be calibrated with an uncertainty of ± 2 %.

5.5 Confirmation of Discussed Uncertainties by Comparative Measurements

Comparison with respect to blackbody radiation. In order to confirm the estimated uncertainties of the vuv spectral radiance calibration procedure a deuterium lamp which was calibrated as described has been compared with a calibrated tungsten strip lamp in the near uv. For the calibration of the strip lamp a tungsten tube blackbody having a temperature of about 2 500 K (MAGDEBURG and SCHLEY [22]) has been used. The temperature of the tungsten tube blackbody has been measured by an indirect radiometric comparison with a graphite blackbody operated at the fixed point temperature of gold with respect to the IPTS 68 (JUNG [25]). The relative uncertainty of the spectral radiance of the tungsten strip lamp due to this procedure is 10^{-2} from 290 nm to 390 nm and $0.6 \cdot 10^{-2}$ from 400 nm to 1000 nm (see also [26]).

In Fig. 12 the ratio $L_{\lambda}^{DL}(Sy)/L_{\lambda}^{DL}(TSL)$ is plotted over the wavelength, where $L_{\lambda}^{DL}(Sy)$ means the spectral radiance of the used deuterium lamp based on the calibration procedure by synchrotron radiation as discussed in this paper and $L_{\lambda}^{DL}(TSL)$ that based on blackbody calibrated tungsten strip lamp radiation.

$L_{\lambda}^{DL}(Sy)/L_{\lambda}^{DL}(TSL) = 1$ indicates that the calibration procedures by blackbody radiation and by synchrotron radiation yield exactly the same result. Between 290 nm and 340 nm the values of the measured ratio vary between 0.99 and 1.015, their mean value being 1.003. The observed deviation from 1 is consistent with the combined uncertainties of the calibration procedures by synchrotron radiation (± 2 %) and blackbody radiation (± 1 %) which allowed values for the ratio $L_{\lambda}^{DL}(Sy)/L_{\lambda}^{Sy}(TSL)$ between 0.97 and 1.03. In the given spectral region the results of the comparative measurements confirm the estimated uncertainties of the spectral radiance determined by means of synchrotron radiation.

Comparison with respect to the hydrogen continuum. A comparison

between the calibrated deuterium lamps and a hydrogen arc [10] is not sufficient to confirm the uncertainties of the synchrotron calibration procedure, because the latter's uncertainties are significantly smaller than those of the hydrogen arc itself. This comparison appears to be important however, because discrepancies have been reported [15] which are mentioned in section 1.2. The comparison has been performed with the hydrogen arc operated at the Technische Universität München [27]. Fig. 13 shows values of the ratios $L_{\lambda}^{DL}(Sy)/L_{\lambda}^{DL}(H_2\text{-arc})$, where $L_{\lambda}^{DL}(H_2\text{-arc})$ means values of the spectral radiance of a deuterium lamp based on the radiation of the hydrogen arc (uncertainty ± 5 %). For the region between 175 nm and 340 nm the measured values of the ratio $L_{\lambda}^{DL}(Sy)/L_{\lambda}^{DL}(H_2\text{-arc})$ vary between 0.97 and 1.07, their mean value being 1.03. The observed deviation from 1 is consistent with the combined uncertainties of both calibration procedures which allowed values between 0.93 and 1.07. The hydrogen continuum may thus be considered to be calculable within the given uncertainties. This result is additionally confirmed by a just terminated laboratory intercomparison between the NBS, the MPI für Astronomie (Heidelberg), and the PTB with respect to a relative spectral radiance scale [28].

References

[1] E. Hinnov, Report MATT - 1022, Princeton University, February 1972

[2] D. Stuck and B. Wende, Phys. Rev. 9A, 1 (1974)

[3] D. Stuck and B. Wende, Temperature. Its Measurement and Control in Science and Industry, Vol. 4, Part 1, p. 105. Instrument Society of America, Pittsburg 1972

[4] B. Wende, Proc. Europ. Conf. on Temperature Measurement, Inst. Phys. Conf. Ser. No. 26, 358. The Institute of Physics, London 1975

[5] H. Nubbemeyer, D. Stuck and B. Wende, Comité Consultatif de Thermométrie, 9. Session 6. - 7. July, 1971, BIPM

[6] L. R. Canfield, R. G. Johnston, and R. P. Madden, Appl. Opt. 12, 1611 (1973)

[7] E. Pitz, Appl. Opt. 8, 255 (1969)

[8] G. Boldt, Space Sci. Rev. 11, 728 (1970)

[9] D. Stuck and B. Wende, J. Opt. Soc. Am. 62, 96 (1972)

[10] W. R. Ott, K. Behringer, and G. Gieres, Appl. Opt. 14, 2121 (1975)

[11] W. C. Griffin and R. W. P. McWhirter, Proc. Conf. Opt. Instr. (London, Chapman and Rall, 1962) 14 ff

[12] D. Lemke and D. Labs, Appl. Opt. 6, 1043 (1967)

[13] P. J. Key, Int. J. Scient. Metrology 6, 97 (1970)

[14] H. Kaase, Journal of Physics E 8, 590 (1975)
H. Kaase, Optik 46, 149 (1976)

[15] W. R. Ott and J. D. Bartoe, Annual Meeting Optical Society of America (1972), Th F 13

[16] J. Schwinger, Phys. Rev. 75, 1912 (1949)

[17] R. Haensel and C. Kunz, Z. angew. Physik 23, 276 (1967)

[18] R. P. Madden "Synchrotron Radiation and Application in x-ray spectroscopy" ed. by L. Azaroff, McGraw Hill, New York (1974)

[19] F. G. Schneider, Phys. Rev. 49, 341 (1936)

[20] J. A. R. Samson, Techniques in vacuum ultraviolet spectroscopy (New York, Wiley, 1967)

[21] D. Einfeld and D. Stuck, Opt. Comm. 19, 297 (1976)

[22] H. Magdeburg and U. Schley, Z. angew. Phys. 20, 465 (1966)

[23] H. J. Jung, Z. angew. Phys. 30, 338 (1971)
G. Sauerbrey, Appl. Opt. 11, 2576 (1972)

[24] K. Schurer, Optik 28, 44 (1968/69)

[25] H. J. Jung, Inst. Phys. Conf. Ser. No. 26, 278. The Institute of Physics, London 1975

[26] C. L. Sanders. International Directory of Calibration Services in the Field of Photometry and Radiometry, National Research Council Ottawa, Canada, K 1 A OR 6

[27] D. Einfeld, D. Stuck, K. Behringer and P. Thoma, Z. Naturforsch. 31a, 1131 (1976)

[28] J. M. Bridges, W. R. Ott, E. Pitz, A. Schulz, D. Einfeld and D. Stuck, Appl. Opt., to be published

Table 2

Spectral radiance L_λ^{vuv} of 9 deuterium lamps (group 1 to 4) of same type and manufacturer for $\lambda = 200$ nm and different operating times. The corresponding relative spectral radiances between 165 nm and 340 nm are shown in Fig. 9.

	lamp no.	operating time hours	L_λ $10^{10} Wm^{-3} sr^{-1}$
group 1	D-60F, 1.1	8	8.63
	, 1.2	8	6.65
	, 1.3	8	9.33
group 2	D-60F, X.1	50	5.89
	, X.2	50	5.00
	, X.3	50	6.05
group 3	D-60F, 2.1	150	3.88
	, 2.2	150	4.50
group 4	D-60F, 2.3	180	4.63

Table 1 Properties of the used polarizers

type	measured or calculated degree of polarization p produced by the polarizers		short wavelength transmission limit
	$p \geq 0.99$ for wavelength	$p < 1$ for wavelength	
film polarizer (Käsemann)	λ = 310...650 nm	p = 0.85...1.00 for λ = 275 ...310 nm	λ = 260 nm
film polarizer (Oriel)	λ = 200...230 nm	p = 1.00...0.82 for λ = 230 ...350 nm	λ = 200 nm
LiF pile-of-plate	-	p = 1.00...0.85 for λ = 105 ...350 nm	λ = 105 nm

(c)

contributions to the uncertainty of $F(\lambda)$	$\Delta x_k^{(4)}/x_k^{(4)}$
spatial distribution of the synchrotron electrons in orbit	$\pm 2 \cdot 10^{-3}$
adjustment of apertures 1 and 2	$\pm 6 \cdot 10^{-3}$
electron energy	$\pm 7 \cdot 10^{-4}$
radius of electron orbit	$\pm 4 \cdot 10^{-4}$
degree of polarization produced by the radiometer in the vis	$\pm 6 \cdot 10^{-3}$
degree of polarization produced by the radiometer in the vuv	$\pm 1 \cdot 10^{-2}$

$\Delta y_4/y_4 = \pm 1.4 \cdot 10^{-2}$

(d) uncertainty of L_λ^{TSL} for $\lambda_o = 458$ nm $\Delta y_5/y_5 = \pm 8 \cdot 10^{-3}$

(e) result

relative uncertainty $\Delta L_\lambda^{vuv} / L_\lambda^{vuv} = \pm 1.8 \cdot 10^{-2}$

Table 3

Relative uncertainty contributions of $\frac{\Delta y_i}{y_i} = \left\{ \sum_i \left(\frac{\Delta x_k^{(i)}}{x_k^{(i)}} \right)^2 \right\}^{1/2}$ to the measured radiance L_λ^{vuv} between 165 nm and 350 nm according to Eq. 5

(a) uncertainty of $i^{Sy}(\lambda_o)/i^{Sy}(\lambda)$ $\Delta y_1/y_1 = \pm 1 \cdot 10^{-3}$

(stray light, radiation of higher orders)

(b)

contributions to the uncertainties of $i^{vuv}(\lambda)$ and $i^{vis}(\lambda_o)$ respectively which have the same amount	$\Delta x_k^{(2,3)}/x_k^{(2,3)}$
non-linearity and drift of the photomultipliers	$\pm 1.5 \cdot 10^{-3}$
non-linearity and drift of the device for measuring photomultiplier currents	$\pm 1 \cdot 10^{-3}$
different size of the irradiated grating surfaces	$\pm 4 \cdot 10^{-3}$
diffraction	$\pm 5 \cdot 10^{-3}$
stray light, radiation of higher orders	$\pm 1 \cdot 10^{-3}$

vis-channel: $\Delta y_2/y_2 = 7 \cdot 10^{-3}$

vuv-channel: $\Delta y_3/y_3 = 7 \cdot 10^{-3}$

Figures

Fig. 1: Schematic representation of the used calibration procedure by means of electron synchrotron radiation.

Fig. 2: Computed spectral radiant power Φ_λ^{Sy} of synchrotron radiation over the azimuthal angle ψ and the position z respectively. Φ_λ^{Sy} is the mean value taken over the time $t_2 - t_1 = 2$ ms of that part of the synchrotron radiation passing through aperture 1 as shown in Fig. 1 Integration starts at $t_1 = 4$ ms after injection of the electrons to be accelerated. The averaged electron current assumed for calculation is 10 mA corresponding to $6.6 \cdot 10^{10}$ electrons in orbit. The radius of the electron orbit is R = 31.72 m. The final energy of the electrons amounts to 6 GeV.

Fig. 3: Mean values of the degree of polarization $p^{Sy}(\lambda)$ of the synchrotron radiation passing through aperture 1 over the azimuthal angle ψ and the position z respectively computed under the same conditions as given in Fig. 2.

Fig. 4: Function $F(\lambda)$ for final energies between 1.7 GeV and 7.2 GeV computed for the position of aperture 1 (vis-aperture) z = 6 mm and that of aperture 2 (vuv-aperture) z = -18 mm (compare Fig. 7). The wavelength in the visible λ_0 is chosen to be 458 nm. All further conditions are the same as given in Fig. 2.

Fig. 5: Arrangement for the calibration of radiometric transfer standards in the uv and vuv spectral region by means of synchrotron radiation. The z-direction is perpendicular to the plane defined by the entrance pinhole and the centers of the concave mirror, gratings, and exit slits.

Fig. 6: a) Photomultiplier current i(t) produced by the synchrotron radiation pulses. The gate time is usually $\Delta t = 2$ ms, the delay time $\Delta t' = 4$ms.

b) Block diagram of the electronic device for measuring the photomultiplier current i(t).

Fig. 7: Photographs of the available synchrotron radiation field (white area).

a: if the shutter is not used to block out the x-ray radiation propagating in the vicinity of the synchrotron orbital plane

b: if the shutter is used.

Fig. 8: Degree of polarization produced by the optical elements of the vuv-channel $p^{vuv}(\lambda)$ and of the vis-channel $p^{vis}(\lambda)$ of the radiometer measured with different polarizers (two different types of film polarizers and a LiF-pile of plates).

Fig. 9: Relative spectral radiances of three deuterium lamps D-60 F (Quarzlampengesellschaft mbH, Hanau, Germany), numbered X 1...X 3, which had been purchased at the same time and had the same number of operating hours (50 hours). Operating parameters are: current of the discharge 300 mA, heating current 3.5 A, solid angle of the measured radiation $2.7 \cdot 10^{-5}$ sr, circular emitting area, diameter 0.9 mm.

Fig. 10: Mean values of the relative spectral radiances of the deuterium lamps listed in Tab. 2 with different number of operating hours: 8 h(3 lamps), 50 h (3 lamps), 150 h (2 lamps), 180 h (1 lamp).

Fig. 11: Comparison of the relative spectral radiances of two different types of deuterium lamps D-15 and D-60 F from the same manufacturer (Quarzlampengesellschaft mbH, Hanau, Germany).

Fig. 12: Ratio $L_\lambda^{DL}(Sy)/L_\lambda^{DL}(TSL)$ of spectral radiances due to two different calibration procedures in the near uv. $L_\lambda^{DL}(Sy)$ is the spectral radiance of a deuterium lamp based on the calibration procedure by synchrotron radiation described in this paper and $L_\lambda^{DL}(TSL)$ that based on the comparison with a blackbody-calibrated tungsten strip lamp.

Fig. 13: Ratio $L_\lambda^{DL}(Sy)/L_\lambda^{DL}(H_2\text{-arc})$ between 175 nm and 340 nm. $L_\lambda^{DL}(Sy)$ is the spectral radiance of a deuterium lamp based on synchrotron radiation, $L_\lambda^{DL}(H_2\text{-arc})$ that based on the hydrogen continuum of a wall stabilized arc.

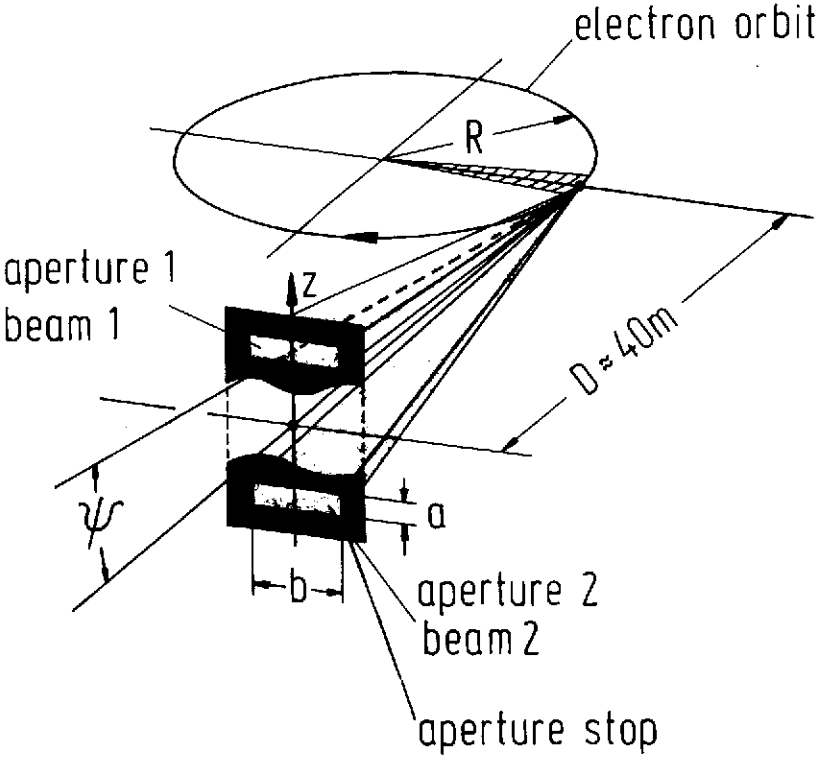

Abb. 1

Einfeld, Stuck, Wende

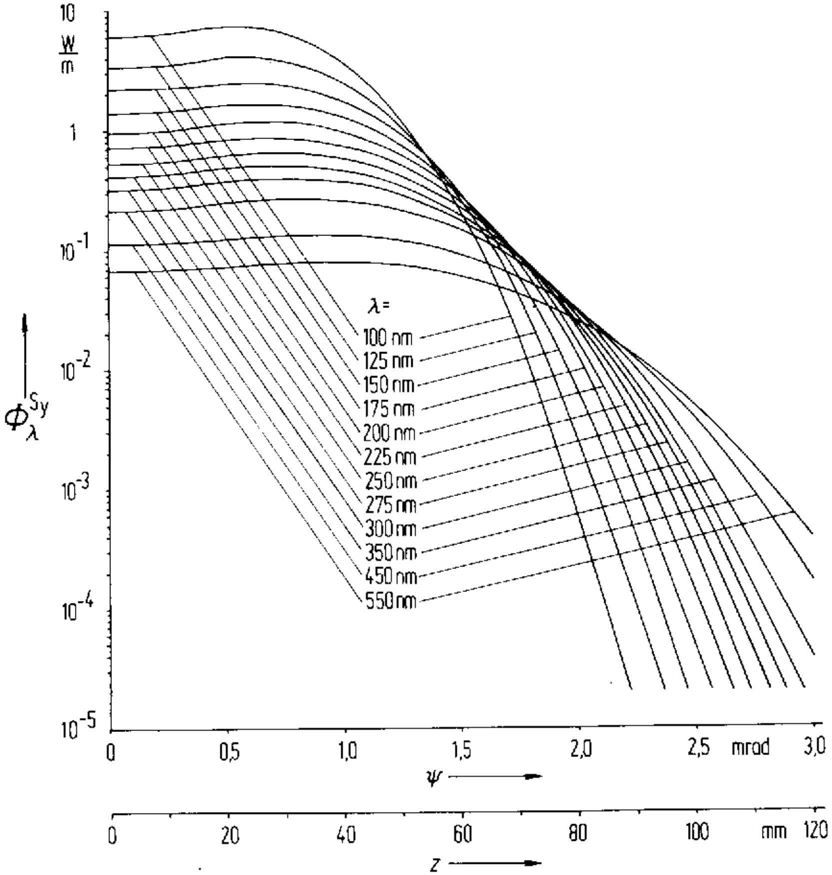

Abb. 2

Einfeld, Stuck, Wende

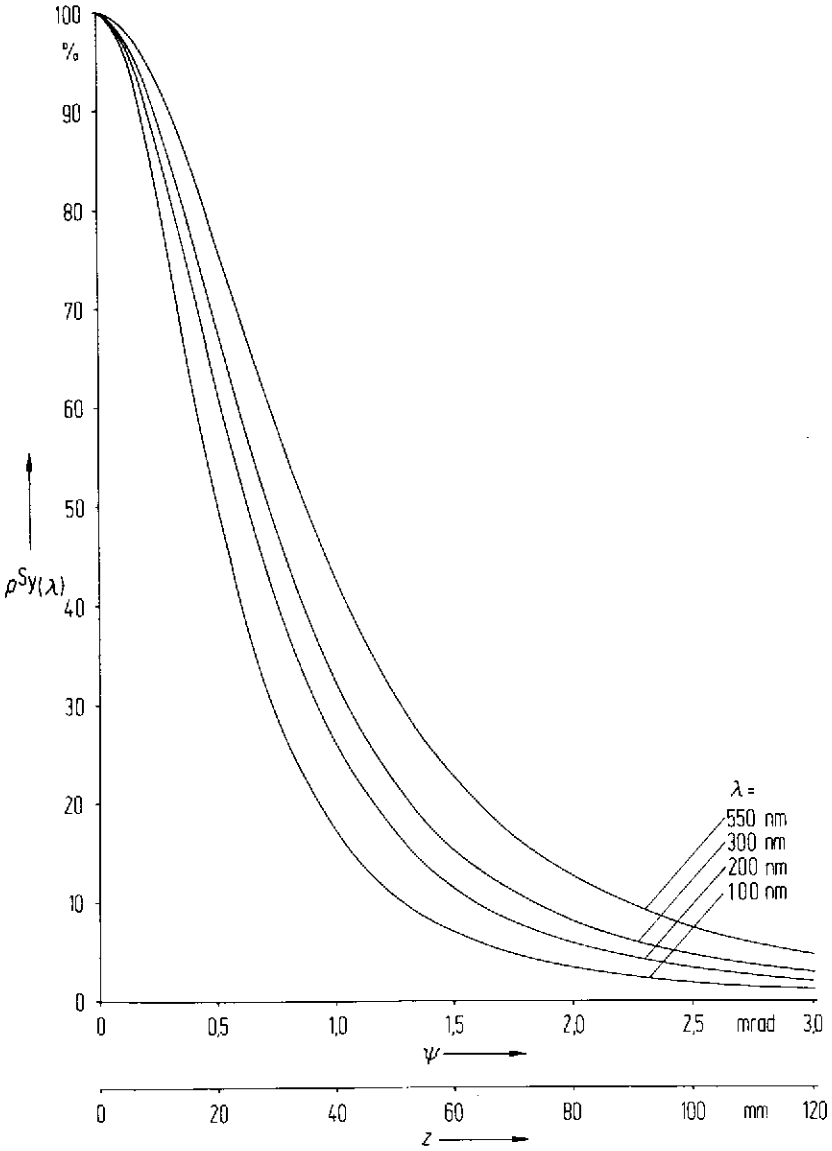

Abb. 3

Einfeld, Stuck, Wende

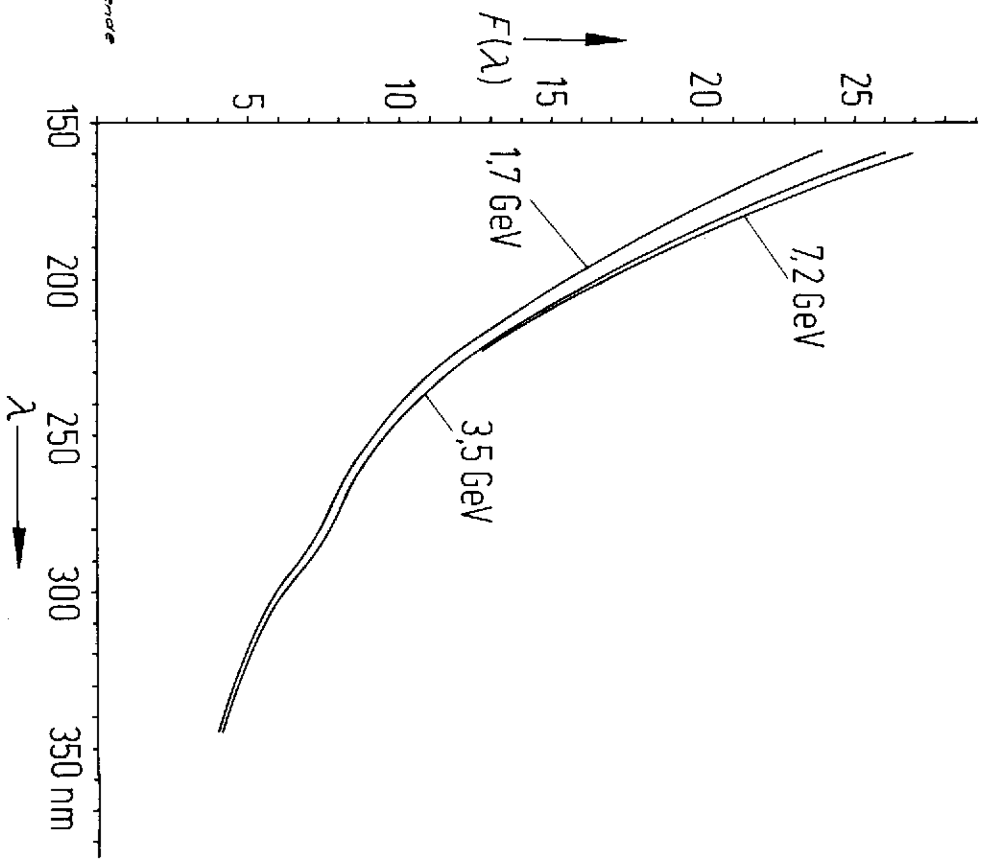

Abb. 4

Einfeld, Stuck, Wende

Abb. 5

Einfeld, Stuck, Wende

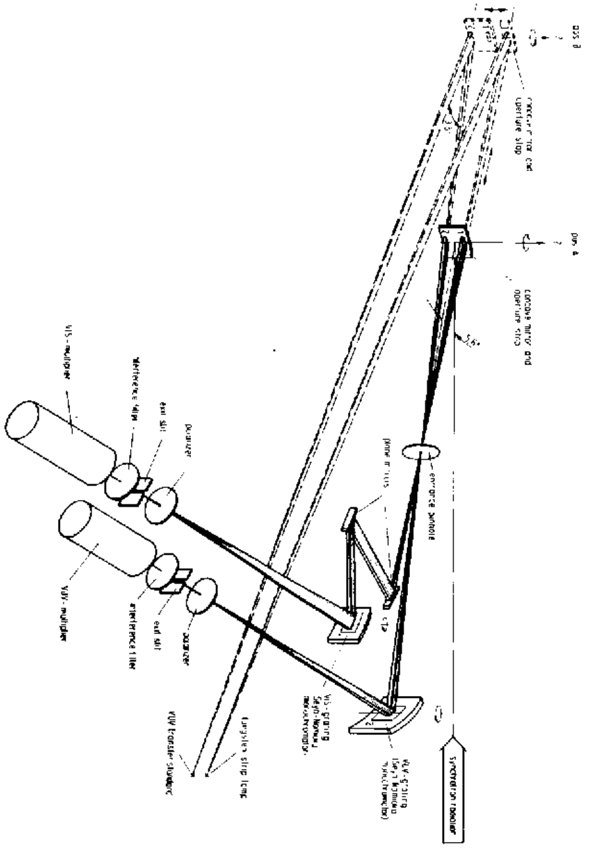

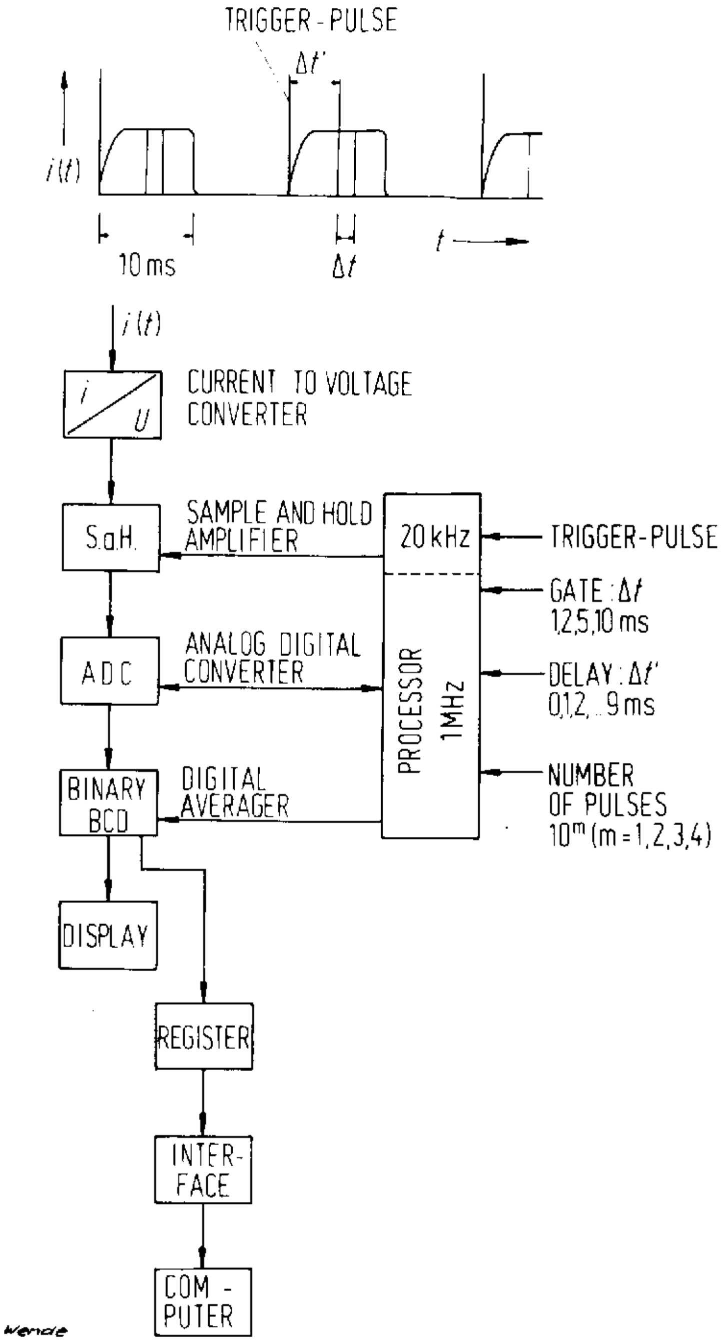

Abb. 6

Einfeld, Stuck, Wende

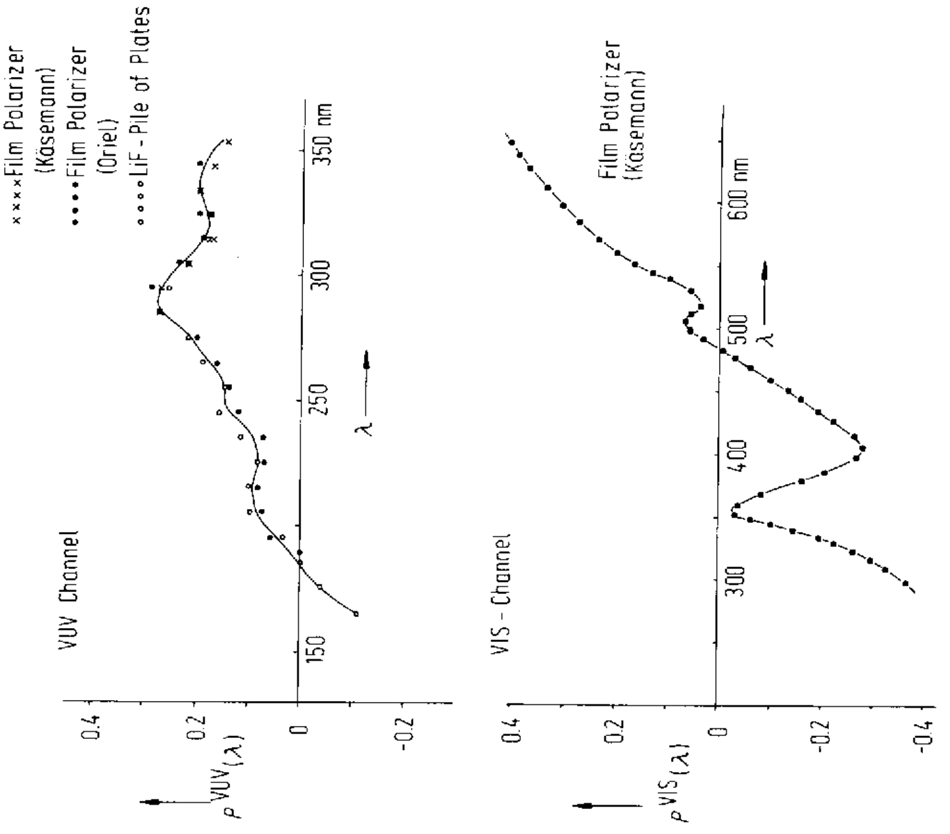

Abb. 8
Einfeld, Stuck, Wende

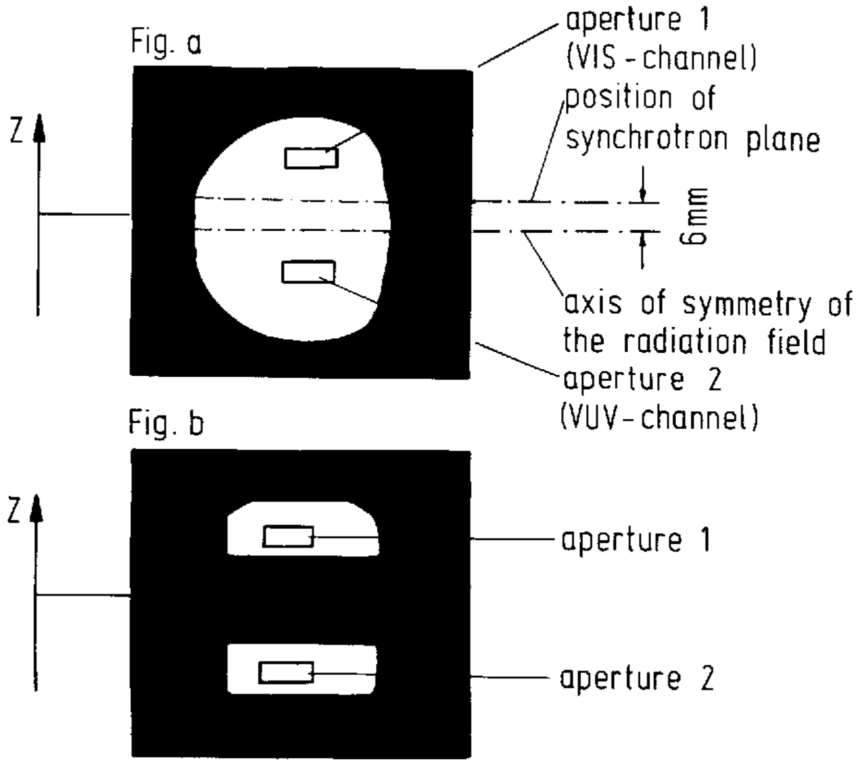

Abb. 7
Einfeld, Stuck, Wende

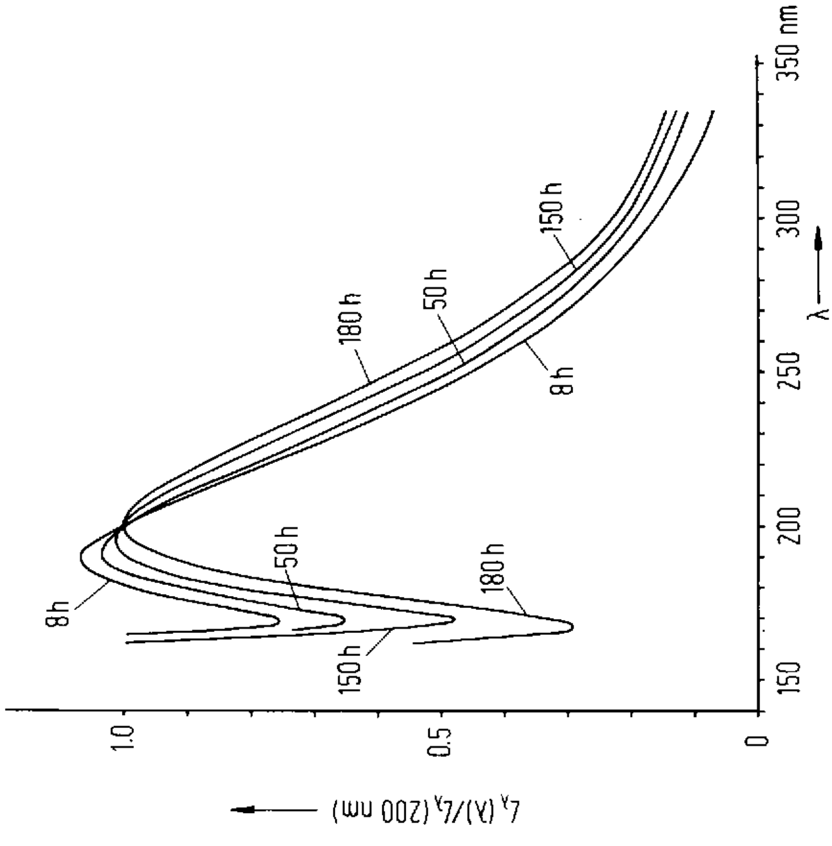

Abb. 10
Einfeld, Stuck, Wende

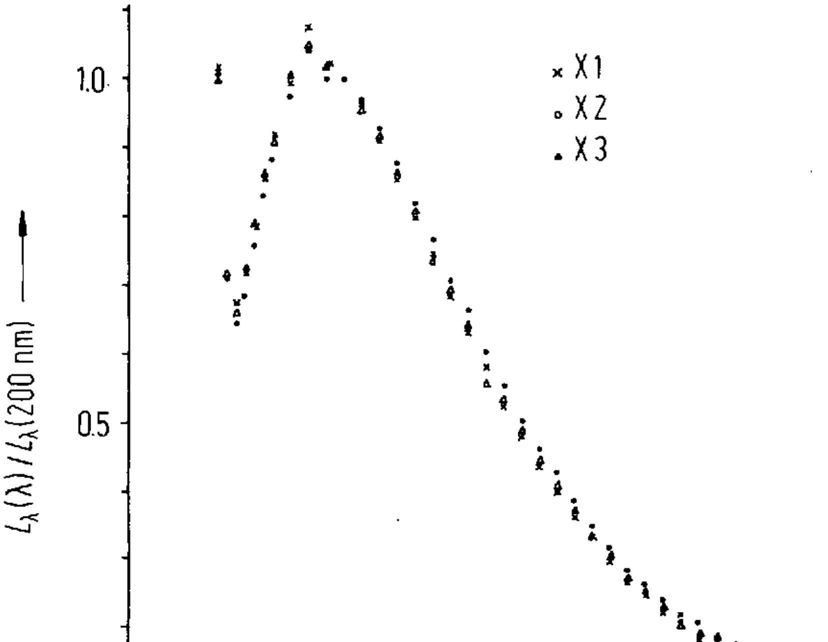

Abb. 9
Einfeld, Stuck, Wende

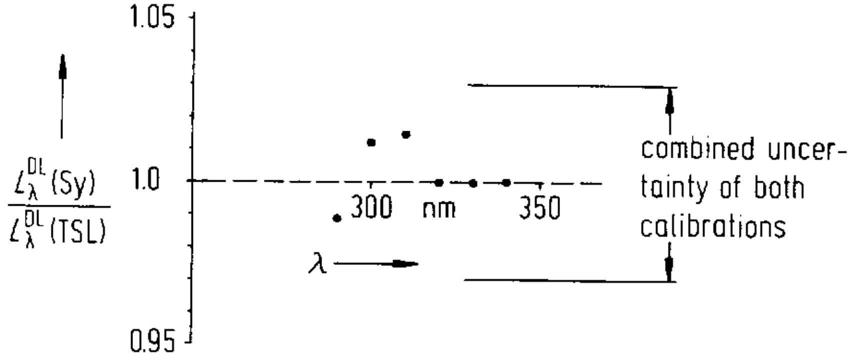

Abb. 12
Einfeld, Stuck, Wende

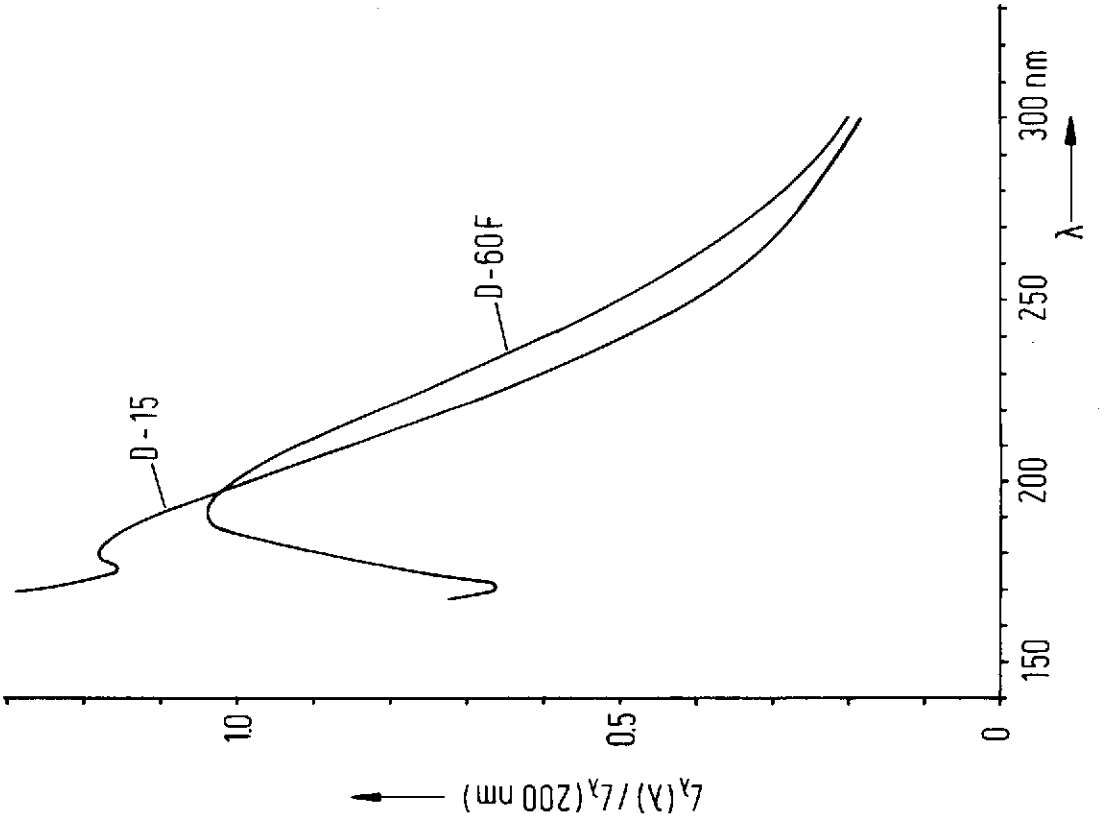

Abb. 11
Einfeld, Stuck, Wende

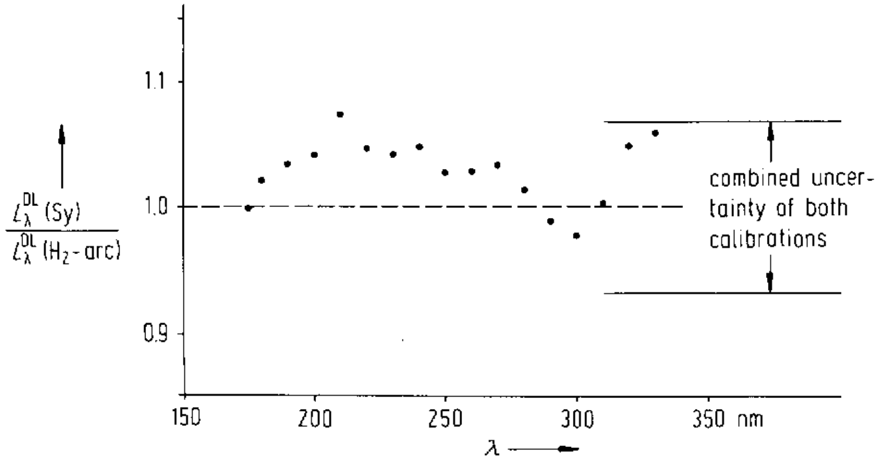

Abb. 13

Einfeld, Stuck, Wende